551. 511. 32:
551. 515. 1

AN INVESTIGATION OF THE SURFACE PRESSURE TENDENCIES AND A VORTICITY BUDGET FOR A CYCLONE DEVELOPMENT

by

LENNART BENGTSSON

Institute of Meteorology, University of Uppsala[1])

Abstract

PETTERSSEN's extension of SUTCLIFFE's theory of development at sea level has carefully been studied, and a quantitative computation of the different terms in the development equation has been performed during some phases in a rapid cyclogenesis. The vertical motion is computed from a two-parameter model under the assumption of quasi-geostrophic, frictionless and adiabatic flow. The vorticity generated by the condensation heat is computed over an area around the sea-level cyclon and contributes very much to the development. A special attention is also paid to the twisting effect and the vertical advection of vorticity. The development of a storm which occurred in North-West Europe during the period August 1—2. 1958, is investigated.

1. *Introduction*

In 1955 PETTERSSEN [7] and PETTERSSEN *et al.* [8] published a theoretical and an experimental investigation on the problem of cyclone development at sea level. The concept of development has been used in Sutcliffe's terminology (SUTCLIFFE [9]). A rather complicated formula can be derived from the vorticity equation and the first law of thermo-

[1]) Now at the Swedish Meteorological and Hydrological Institute, Stockholm.

dynamics, which expresses the local vorticity variation at the 1000-mb level as an unbalance between the local vorticity variation of the lowest level of non-divergence and the Laplacian of the local variation of the thermal vorticity field between the 1000-mb level and the level of non-divergence. The Laplacian of the thermal vorticity field can be written in terms including advection of thickness lines, vertical motions, stability and non-adiabatic processes. In former studies of this kind the vertical advection of vorticity and the so called twisting-term have been omitted. In this paper they have been considered, and it is likely that in areas with large vertical velocities they will make a large contribution to the vorticity development.

Yet, it must first be pointed out that Petterssen's simplified formula is most suitable for qualitative reasoning, which is due partly to the very complicated form of the development equation, and partly to the fact that the different terms are not physically independent. However, the advectional terms, which as a rule are the most important ones, are simple to compute, and several storms have been investigated by a calculation of them (FUGE [4], MEANS [5] and [6]). The assumption of a constant level of non-divergence is also very crude, since we know that this level performs great excursions in the vertical in connection with cyclogeneses. Further, ageostrophic winds and friction, omitted in the equations, play an important rôle in areas of cyclonic development.

In this investigation the vertical motions are computed with the aid of a two parameter model used for the numerical prediction which does not include the effect of non-adiabatic heating, variable stability, geostrophic departures and friction. Consequently, they should be treated with great caution. The vertical velocities have been studied in relation to the surface weather maps and seem to be of approximately the correct order of magnitude and to have the correct sign (fig. 1). Nevertheless, in areas with precipitation, the latent heat from the condensation processes will initiate non-adiabatic vertical velocities which can at times greatly surpass the velocities computed from an adiabatic model (BANNON [2], VUORELA [11]).

An attempt has been made to compute the different terms in eq. (2.23) during a rapid cyclogenesis occuring in August 1958 and to study the relative magnitude of the factors influencing the development at sea level.

The main reason why a study of a case of summer cyclogenesis has been undertaken is that the flux of sensible heat is comparatively small

at that time of the year, so that the heat source in this storm is essentially assumed to be the condensation heat.

We will first derive a development equation which is used in the computations, and efter that shortly describe the synoptic situation.

2. *Derivation of the development equation*

If we assume as vertical boundary condition that $\omega = \frac{dp}{dt} = 0$ for $p = 0$ and $p = p_0$, it follows that there is at least one value for p where $\frac{\partial \omega}{\partial p} = 0$ in the interval $0 \leq p \leq p_0$. According to the equation of continuity, this also means that $\nabla_2 \mathbf{v} = 0$. We will in the following make use of the 500-mb level as the lowest level of non-divergence. This is of course not exact, but it seems anyhow to be the best approximation.

We write first the vorticity equation at the level of non-divergence. (Quantities at the 500-mb level are denoted by the subscript L, while quantities at the surface of the earth are denoted by subscript O.)

$$\frac{\partial \xi_L}{\partial t} + \mathbf{v}_L \cdot \nabla \eta_L + \omega_L \frac{\partial \xi_L}{\partial p} = \mathbf{k} \cdot \left(\frac{\partial \mathbf{v}_L}{\partial p} \times \nabla \omega_L \right) \tag{2.1}$$

$\xi = \mathbf{k} \cdot \nabla \times \mathbf{v}$ represents the relative vorticity and $\mathbf{k}$ the unit vector directed upward. $\eta = \xi + f$, where f is the Coriolis parameter.

We have also that $\mathbf{v}_T = \mathbf{v}_L - \mathbf{v}_0$ where $\mathbf{v}_T$ is the thermal wind. From this: $\xi_T = \mathbf{k} \cdot \nabla \times \mathbf{v}_T = \xi_L - \xi_0$.

If we make use of this expression for ξ_T and furthermore perform the vector multiplication for the so called twisting-term we get:

$$\frac{\partial \xi_0}{\partial t} = -\frac{\partial \xi_T}{\partial t} - \mathbf{v}_L \cdot \nabla \eta_L - \omega_L \frac{\partial \xi_L}{\partial p} + \frac{\partial u_L}{\partial p} \cdot \frac{\partial \omega_L}{\partial y} - \frac{\partial v_L}{\partial p} \cdot \frac{\partial \omega_L}{\partial x} \tag{2.2}$$

where u is the velocity in easterly direction and v in northerly direction.

We now wish to express the local variation of the thermal vorticity, the vertical advection of vorticity and the twisting term in such a way that it will be possible to get a physcial interpretation of these factors, and also express them in parameters which we can obtain from ordinary weather maps.

We shall in the following make use of:

$$\frac{dQ}{dt} = c_p \frac{dT}{dt} + \alpha \frac{dp}{dt} \qquad \text{(the first law of thermodynamics)} \tag{2.3}$$

$$p\alpha - RT = 0 \qquad \text{(the equation of state)} \qquad (2.4)$$

$$\Theta = T\left(\frac{p}{p_0}\right)^{-\frac{R}{c_p}} \qquad \text{(potential temperature relationship)} \qquad (2.5)$$

Here Q is the heat energy; c_p, specific heat at constant pressure; α, specific volume and R the gas constant for dry air.

We also use some approximations:

$$\frac{\partial p}{\partial z} + \frac{g}{\alpha} = 0 \qquad \text{(Hydrostatic equation)} \qquad (2.6)$$

$$\mathbf{v}_g = \frac{g}{f}\,\mathbf{k} \times \nabla z \qquad \text{(geostrophic relation)} \qquad (2.7)$$

$$F = 0 \qquad \text{(no friction)} \qquad (2.8)$$

In order to get a tractable form for the local variation of thermal vorticity we shall use the same technic as demonstrated by PETTERSSEN [7]. With the aid of eqs. (2.4), (2.5) and (2.6), the first law of thermodynamics (2.3) can be written in the following way:

$$\frac{\partial}{\partial t}\left(g\frac{\partial z}{\partial p}\right) = -\mathbf{v}\cdot\nabla\left(g\frac{\partial z}{\partial p}\right) - \omega\frac{R}{p}\left(\frac{\partial T}{\partial p} - \frac{R}{c_p}\frac{T}{p}\right) - \frac{R}{c_p p}\frac{dQ}{dt} \qquad (2.9)$$

Identifying the term in the second bracket on the right side we see that:

$$\frac{\partial T}{\partial p} = \Gamma \qquad \text{(actual lapse rate in } xypt\text{-system)} \qquad (2.10)$$

$$\frac{RT}{c_p p} = \Gamma_d \qquad \text{(dry adiabatic lapse rate)} \qquad (2.11)$$

We now get:

$$\frac{\partial}{\partial t}\left(g\frac{\partial z}{\partial p}\right) = -\mathbf{v}\cdot\nabla\left(g\frac{\partial z}{\partial p}\right) + \frac{R}{p}\omega(\Gamma_d - \Gamma) - \frac{R}{c_p\cdot p} - \frac{dQ}{dt} \qquad (2.12)$$

If we finally integrate this equation from p_0 to p_L we get

$$g\frac{\partial z_T}{\partial t} = \int_{p_L}^{p_0}\mathbf{v}\cdot\nabla\left(g\frac{\partial z}{\partial p}\right)dp - R\int_{p_L}^{p_0}\omega(\Gamma_d - \Gamma)\frac{dp}{p} + \frac{R}{c_p}\int_{p_L}^{p_0}\frac{dQ}{dt}\frac{dp}{p} \qquad (2.13)$$

$$g\frac{\partial z_T}{\partial t} = (p_0 - p_L)\,\overline{\mathbf{v}\cdot\nabla\left(g\frac{\partial z}{\partial p}\right)} - R\ln\frac{p_0}{p_L}\,\widetilde{\omega(\Gamma_d - \Gamma)} + \frac{R}{c_p}\ln\frac{p_0}{p_L}\,\widetilde{\frac{dQ}{dt}} \quad (2.14)$$

The mean quantities are defined:

$$\overline{(\quad)} = \frac{1}{p_0 - p_L}\int_{p_L}^{p_0}(\quad)\,dp \quad (2.15)$$

$$\widetilde{(\quad)} = \frac{1}{\ln\frac{p_0}{p_L}}\int_{p_L}^{p_0}(\quad)\,d(\ln p) \quad (2.16)$$

Tests with simple functions show that with an error less than some per cent we can replace $\widetilde{(\quad)}$ by $\overline{(\quad)}$.

The deviation from the mean value, with respect to p, for the parameters in eq. (2.14) has been excluded, as there is a very small correlation between them.

Consequently:

$$\overline{\mathbf{v}\cdot\nabla\left(g\frac{\partial z}{\partial p}\right)} = \bar{\mathbf{v}}\cdot\overline{\nabla\left(g\frac{\partial z}{\partial p}\right)} \sim -\frac{1}{p_0 - p_L}\,\bar{\mathbf{v}}\cdot\nabla(gz_T)\,;\; z_T = z_L - z_0 \quad (2.17)$$

$$\overline{\omega(\Gamma_d - \Gamma)} = \bar{\omega}\overline{(\Gamma_d - \Gamma)} \quad (2.18)$$

Inserting in (2.14) we get:

$$\frac{\partial z_T}{\partial t} = -\bar{\mathbf{v}}\cdot\nabla z_T - \frac{R}{g}\ln\frac{p_0}{p_L}\,\bar{\omega}\overline{(\Gamma_d - \Gamma)} + \frac{R}{gc_p}\ln\frac{p_0}{p_L}\,\overline{\frac{dQ}{dt}} \quad (2.19)$$

Here we can in accordance with Petterssen introduce the pseudo-adiabatic lapse rate for saturated air, Γ_s. If all the released heat is taken up by the dry air and if we further put $p - e_s \sim p$, where e_s is the vapor pressure, we arrive at the following form of the first law of thermodynamics:

$$-L\,dr = c_p dT - RT\frac{dp}{p}$$

where L is the latent heat of evaporation and r is the condensed water vapor.

After some manipulations we get

$$\Gamma_s - \Gamma_d = -\frac{L}{c_p}\frac{dr}{dt}\frac{dt}{dp} \quad \text{where} \quad \Gamma_s = \left(\frac{\partial T}{\partial p}\right)_{Q \neq 0}$$

or

$$\overline{\omega\Gamma_d} = \overline{\omega\Gamma_s} + \frac{L}{c_p}\overline{\frac{dr}{dt}} ,$$

$\overline{\frac{dr}{dt}}$ may be interpreted as the rate of precipitation and $L\overline{\frac{dr}{dt}}$ as the non-adiabatic heat arising from the condensation processes.

If we insert this in (3.19) we get

$$\frac{\partial z_T}{\partial t} = -\mathbf{v}\cdot\nabla z_T - \frac{R}{g}\ln\frac{p_0}{p_L}\overline{\omega(\Gamma_s - \Gamma)} + \frac{R}{gc_p}\ln\frac{p_0}{p_L}\overline{\frac{dQ'}{dt}} \qquad (2.19)'$$

We must here observe that the condensation heat is introduced in the vertical motion-stability term or the »buoyancy» term. Q is the remaining heat energy, when the latent heat has been removed.

Excluding variation of the Coriolis parameter, the expression for the geostrophic vorticity is:

$$\xi = \frac{g}{f_0}\nabla^2 z$$

From this we obtain:

$$\frac{\partial \xi_T}{\partial t} = \frac{g}{f_0}\nabla^2\left[-\bar{\mathbf{v}}\cdot\nabla z_T - \frac{R}{g}\ln\frac{p_0}{p_L}\overline{\omega(\Gamma_d - \Gamma)} + \frac{R}{gc_p}\ln\frac{p_0}{p_L}\overline{\frac{dQ}{dt}}\right] \qquad (2.20)$$

The vertical advection of vorticity can be written with the aid of (3.6) and (3.7) in the following way:

$$\omega\frac{\partial \xi_L}{\partial p} = -\frac{R}{f_0 p_L}\omega_L\nabla^2 T_L \qquad (2.21)$$

And the twisting term:

$$\frac{\partial u_L}{\partial p}\cdot\frac{\partial \omega_L}{\partial y} = \frac{\partial v_L}{\partial p}\cdot\frac{\partial \omega_L}{\partial x} = +\frac{R}{f_0 p_L}\left[\frac{\partial T_L}{\partial y}\cdot\frac{\partial \omega_L}{\partial y} + \frac{\partial T_L}{\partial x}\cdot\frac{\partial \omega_L}{\partial x}\right] \qquad (2.22)$$

Inserting the expressions (2.20), (2.21) and (2.22) in eq. (2.2) we get the total development equation:

$$\frac{\partial \xi_0}{\partial t} = - \mathbf{v}_L \cdot \nabla \eta_L + \frac{g}{f_0} \nabla^2 \left[\bar{\mathbf{v}} \cdot \nabla z_T + \frac{R}{g} \ln \frac{p_0}{p_L} \overline{\omega (\overline{\Gamma_d - \Gamma})} - \right.$$
$$\left. - \frac{R}{g c_p} \ln \frac{p_0}{p_L} \overline{\frac{dQ}{dt}} \right] + \frac{R}{f_0 p_L} \left[\omega_L \nabla^2 T_L + \right. \tag{2.23}$$
$$\left. + \left(\frac{\partial T_L}{\partial x} \cdot \frac{\partial \omega_L}{\partial x} + \frac{\partial T_L}{\partial y} \cdot \frac{\partial \omega_L}{\partial y} \right) \right].$$

$$\frac{\partial \xi_0}{\partial t} = - \mathbf{v}_L \cdot \nabla \eta_L + \frac{g}{f_0} \nabla^2 \left[\bar{\mathbf{v}} \cdot \nabla z_T + \frac{R}{g} \ln \frac{p_0}{p_L} \overline{\omega (\overline{\Gamma_s - \Gamma})} - \right.$$
$$\left. - \frac{R}{g c_p} \ln \frac{p_0}{p_L} \overline{\frac{dQ'}{dt}} \right] + \frac{R}{f_0 p_L} \left[\omega_L \nabla^2 T_L + \right. \tag{2.23'}$$
$$\left. + \left(\frac{\partial T_L}{\partial x} \cdot \frac{\partial \omega_L}{\partial x} + \frac{\partial T_L}{\partial y} \cdot \frac{\partial \omega_L}{\partial y} \right) \right].$$

3. *General synopsis*

The cyclogenesis of August 1—2. 1958 was one of those intense summer developments that are rather unusual. In the early morning of August 2 the pressure fell 10 mb in 6 hours at the center of the low, and great amounts of precipitation were measured over large areas in the central parts of Sweden (25—45 mm in 12 hours). What was the pre-history of this dramatic occurrence?

During the last days of July small stable waves were moving on a westerly track from the Azores over the Pyrenees to the Black Sea. One of these waves laid in the morning of July 31 off the coast of Portugal and took contrary to its forerunners a course to northeast. The reason for this change of direction was an impulse from a northerly jet stream east of Greenland which involved a sharpening and intensifying of the main trough over the North Atlantic and probably initiated a creation of a surface low west of Ireland. On August 1 the polar front over western Europe got more and more well-defined, and the surface disturbance continued its northeasterly course slowly deepening into a closed low.

As the main trough line of the basic current turned counterclockwise, the surface low west of Ireland moved towards the North Sea and the precipitation areas of the two surface lows gradually fused. The baroclinicity of the basic current increased and intensified the thermal advection, see figs. 4c, 5c and 6c. In spite of the intensification of the isallobaric

field during August 1 no grater increase in the circulations around the low was observed. Not until the core of the vorticity advection of the 500-mb field was superimposed upon the sea-level low (fig. 5b) did the rapid increase in circulation take place, combined with an »explosive» deepening. Consequently, this case is a new verification of Petterssen's hypothesis, which states that a region of appreciable low-level convergence results when an area of appreciable positive vorticity advection superimposes a weak surface low.

The deepening of this cyclone seemed to start at sea-level, compare for example the sea-level map for 12 z, August 2, with the 500-mb map for the same time. (Still no closed circulation is observed on the higher level.) Later on an intense vortex also occurred in the middle and higher parts of the troposphere. After the rapid development in the morning of August 2 the cyclone continued its northeasterly track, but the rate of deepening was after this »accident» very small. The next day the low started to fill in over the North of Scandinavia.

4. *Technique of computation*

In the first part of this study the 3-hours height changes of the 1000-mb contour lines have been computed from a) eqs. (2.19) and (2.19)' to obtain the contribution from the thickness field 1000—500 mb; and b) by an integration of the eq.:

$$\frac{\partial \xi_L}{\partial t} = - \mathbf{v}_L \cdot \nabla \eta_L \tag{4.1}$$

to get the contribution from the vorticity advection at the level of non-divergence. The integration has been performed by Fjörtoft's graphical method (FJÖRTOFT [3]) with a grid distance of $3 \cdot 10^5$ m.

The changes as a consequence of thermal advection have been computed by advection of the thickness field in a smoothed 700-mb field, where waves with a wavelength less than $3 \cdot 10^5$ m have been smoothed out. This may be considered as consistent with a 3-hours advection.

Three consecutive observation periods have been studied and the results of the computations are given in figs. (3a—3g, 4a—4g, 5a—5g).

The expression for the vertical motion-stability has been evaluated in the following way. The vertical velocities available apply at the 600-mb level according to the model approximations, which further include the assumption that ω has a parabolic distribution with zero points at the

1000- and 200-mb level. If we integrate this parabolic expression with respect to p between $p = 1000$ mb and $p = 500$ mb, we get $\overline{\omega} = 0.75\,\omega_{600}$. Without going beyond the error boundary we can replace ω_{600} with ω_{500} and apply the ω-values obtained from the model at the available 500-mb maps.

The stability, here defined as $\overline{\Gamma_d - \Gamma} = \overline{\frac{\alpha}{c_p}} - \overline{\frac{\partial T}{\partial p}}$, can be computed from a $T \cdot \ln p$-diagram, if we write the expression for Γ_d as an area integral. $\overline{\frac{\partial T}{\partial p}}$ can be evaluated directly. To get rid of the nocturnal ground inversions integration in this case may be performed between $p = 950$ mb and $p = 500$ mb. The expression for the stability will then be:

$$\overline{\Gamma_d - \Gamma} = 1{,}12 + 0{,}024 \cdot t_{500} - 0{,}020 \cdot t_{950} \tag{4.2}$$

where t_n represent degrees Celsius.

A more simplified method can be used in the computation of the stability if we make use of informations at 850 mb instead of 950 mb and let the state at 700 mb represent Γ_d.

$$\Gamma_d = \overline{\frac{\alpha}{c_p}} \sim \frac{R}{c_p}\frac{T_{700}}{p_{700}}$$

In this case we get

$$\Gamma_d - \Gamma = 1.11 - 0.029\,(t_{850} - t_{500}) \tag{4.3}$$

The expression (4.3) deviates rather little from (4.2) and has been used in this study because data is easier available at 850 mb. The maps for 850, 700 and 500 mb have been analysed carefully and $\Gamma_d - \Gamma$ has been computed in every grid point of a quadratic grid-net. The mesh size at the standard latitude was $3 \cdot 10^5$ m.

Because of the complexity of the eqs. (2.23) and (2.23)′ they have only been computed over very small areas. The different terms have been evaluated in the neighbourhood of the surface low in ten grid points for three observation periods. After that the mean of the change of the vorticity per unit time has been computed over a circular area with a radius of $3 \cdot 10^5$ m over the surface low. The result of this is tabulated in Table 1.

Table 1. Mean vorticity change per unit time over a circular area ($r = 300$ km) with centre coinciding with sea level pressure centre. Units: 10^{-9} sec^{-2}.

DATE GMT	$-\mathbf{v}_L \nabla \eta_L$	$\frac{g}{f_0} \nabla^2 \bar{\mathbf{v}} \nabla z_T$	$\frac{R}{f_0} \ln \frac{p_0}{p_L} \nabla^2 \bar{\omega} (\Gamma_d - \Gamma)$	$\frac{R}{f_0} \ln \frac{p_0}{p_L} \nabla^2 \overline{\omega (\Gamma_S - \Gamma)}$	$\frac{R}{f_0 p_L} \omega_L \nabla^2 T_L$	$\frac{R}{f_0 p_L} (\nabla T_L \cdot \nabla \omega_L)$
Aug 1 1200	+1,9	−1,7	−2,3	+0,7	+0,8	−0,1
Aug 2 0000	+3,5	+0,5	−4,7	−0,1	+0,8	+0,2
Aug 2 1200	+3,0	+1,0	−3,5	−0,1	+0,7	−0,1

DATE GMT	Observed change	Computed change (dry case)	Computed change (saturated case)	Contribution from condensation heat
Aug 1 1200	+1,7	−1,4	+1,6	+3,0
Aug 2 0000	+6,0	+0,3	+4,9	+4,6
Aug 2 1200	+4,0	+1,0	+4,4	+3,4

In the computation of the pseudoadiabatic lapse rate values have been obtained from Smithsonian Meteorological Tables, 1951, and respect has been paid to data at 850, 700 and 500 mb.

The vertical advection of vorticity and the twisting effect have been evaluated by means of finite differences in 108 grid points.

$$\frac{R}{f_0 p_L}\,\omega_L \nabla^2 T_L \sim -\,4{,}2\cdot 10^{-12}\, w \nabla^2 T_L\,;\; w = \frac{dz}{dt} \sim -\,\frac{\alpha}{g}\,\omega \qquad (4.4)$$

$$\frac{R}{f_0 p_L}\left[\frac{\partial T_L}{\partial x}\cdot\frac{\partial \omega_L}{\partial x} + \frac{\partial T_L}{\partial y}\frac{\partial \omega_L}{\partial y}\right] \sim -\,10^{-12}[(\Delta T_L)_x(\Delta w_L)_x + (\Delta T_L)_y(\Delta w_L)_y] \qquad (4.5)$$

The vertical advection of vorticity and the twisting term will be discussed in section 6.

5. *Discussion of the results*

Computations according to the description in section 4 have been performed for the eqs. (2.19) and (4.1).

We shall first discuss the 3-hours computed changes at the sea level height field and compare the result with the observed isallobaric field, (figs. 3b, 4b and 5b).

The contribution from the vorticity advection term amounts at the most to 20 m/3 h and the part which is associated with the main trough undergoes only small alterations during the different phases of the storm. When the core of the vorticity advection superimposes the sea level low over the eastern part of Skagerac the rapid cyclogenesis seems to take place. During the whole process of development from 12z August 1 to 12z August 2 we observe a continous turning of the vortex tubes in the area of vorticity advection which has such a result that the vorticity advection itself is counteracted, thus resulting in a slowing down of the movement of the vorticity area at 500 mb. Compare figs. 3b, 4b and 5b with 9a, 10a and 11a. This process will preferably be more accentuated than what follows from figs. 9a, 10a and 11a because of an underestimation of the twisting-term, see section 6.

Figs. 3c, 4c and 5c show the thermal advection between 1000 and 500 mb. This factor is changing very much during the development and increases with a multiple of 4. The agreement with the observed field is rather good and the greatest part of the tendence field consists of thermal advection. The thermal advection is largest ahead and in the rear of the cyclone, and does not contribute much to the vorticity development of the surface low (table 1). Largest computed value exceeds 80 m/3 h.

In the buoyancy term the stability and vertical velocity are included. The mean lapse rate between 850 and 500 mb agrees with the lapse rate

in the standard atmosphere. The buoyancy term has a damping effect on the development (table 1) and always gives a positive contribution to height changes of the 1000 mb field in areas with ascending motions and negative in areas with descending motions. As advective warm air as a rule has an ascending component of motion and advective cold air has a descending one, the buoyancy term generally counteracts the thermal advection. The damping effect from the vertical motion-stability term is so dominating that an addition of vorticity advection, thermal advection and the buoyancy term gives a rise of the 1000-mb contours over the low, figs. 3f, 4f, and 5f, or in terms of vorticity no development (table 1)!

In figs. 3g, 4g and 5g the pseudoadiabatic lapse rate has replaced the dry adiabatic in areas with coherent precipitation and Altostratus-formation. These physical processes indicate that condensation takes place and according to eq. (2.19)′ we will get an estimation of the contribution from the condensation heat by replacing Γ_d with Γ_s in the buoyancy term. In table 1 we find that the vorticity contribution from the latent heat exceeds the contribution from vorticity advection in the vicinity of the low. It is interesting to see that also for extra-tropical cyclones the condensation heat plays such an important rôle. Moreover, the vorticity contribution from the latent heat is underrated in this study as no account has been taken to non-adiabatic vertical velocities.

It may be of some interest to consider the behaviour of the vertical advection of vorticity and the twisting-term during a cyclogenesis and these terms will be discussed in the next section.

6. *The twisting-term and the vertical advection of vorticity*

One property of the complete vorticity equation is that the sum of the twisting-term and the vertical advection of vorticity can be written as the divergence of a continuous vector. This implies that the sum of the two factors will be zero if integrated over a closed surface, for example the complete surface of the earth. This important property has been discussed by Wiin-Nielsen, especially with respect to numerical models (Wiin-Nielsen [12]).

This relationship is also approximately true for smaller areas, for instance in this study, where the area is only 4% of the northern hemisphere. It may also be noticed that each of the terms tends to balance itself as can be seen from table 2. Further it follows from table 2 that the

Table 2. The twisting-term and the vertical advection of vorticity. Units: 10^{-10} sec^{-2}.

Date GMT	Area mean			Abs. max		Area mean for abs. value	
	F_1	F_2	F_1+F_2	F_1	F_2	F_1	F_2
Aug 1 1200	+1,9	−1,4	+0,5	+31,9	−14,5	3,8	2,0
Aug 2 0000	−0,06	0,01	−0,05	−26,0	+ 6,6	2,8	1,0
Aug 2 1200	+0,8	−0,5	+0,3	−21,9	− 4,5	2,2	0,8
Time mean values	+0,8	− 0,6	+0,3			2,9	1,3

$$\frac{R}{f_0 p_L}\omega_L \nabla^2 T_L = F_1$$

$$\frac{R}{f_0 p_L}(\nabla T_L \cdot \nabla \omega_L) = F_2$$

$$\frac{F_2}{F_1} = 0{,}43 \sim 0{,}4$$

total sum of the two factors only represents a very small fraction of their largest computed value.

Nevertheless, over proportionately small regions, particularly in connection with intensive baroclinic zones, they now and again act in the same direction and are here about 1/4 of the horizontal vorticity advection (table 1).

This ratio corresponds to the vertical velocities computed from an adiabatic model of the atmosphere, but we know from precipitation measurements that also the large scale vertical velocities arising from the condensation heat can surpass those computed from a »dry» model with up to one order of magnitude (BANNON [2], VUORELA [11]). It is likely therefore that the contribution from these terms is underestimated in areas of precipitation.

Before we examine the analysed maps, let us first shortly in a qualitative way discuss the vorticity contribution from the two terms in some ideal cases. Consider a frontal zone stretching from west to east, where we may for the sake of simplicity disregard variations in directions parallel to the frontal zone. Let us illustrate the hypothetical trends for the curves of temperature and vertical velocity (fig. 6 and fig. 7). Fig 6 shows the variation of temperature and fig. 7 the variation of the vertical velocity for three different cases:

a) A front with an assumed positive energy conversion; ascending warm air and descending cold air.
b) A front with ascending air in both air masses.
c) A front with descending air in both air masses.

Let us now make use of eq. (2.23).

If we only include the vertical advection of vorticity and the twisting effect and exclude variations with respect to x we get:

$$\frac{\partial \xi_0}{\partial t} = \cdots\cdots \frac{R}{f_0 p_L}\left[\omega_L \frac{\partial^2 T_L}{\partial y^2} + \frac{\partial T_L}{\partial y}\frac{\partial \omega_L}{\partial y}\right] = -c\left[w\frac{\partial^2 T}{\partial y^2} + \frac{\partial T}{\partial y}\frac{\partial w}{\partial y}\right] \quad (6.1)$$

where c is a positive constant and $w = \frac{dz}{dt}$.

The twisting-term will on the whole give a positive contribution for all the three cases in both air masses, but the contribution from the vertical advectional term is shown in fig. 8.

Let us after this qualitative discussion examine the computed vorticity distribution during the storm, which is studied in this paper. Looking at figs. 9a and 11a we will find no particular correlation between the sign of the vorticity contribution and the front. Only in fig. 10a the positive vorticity in the vicinity of the front seems to preponderate over the negative. This incompatibility is naturally due to a different and more complicated form of the horizontal variation of the vertical velocity and inconsistencies in the computation of T and ω. As we know temperature has been obtained directly from the analysed maps, but the vertical velocity has been computed under certain assumptions.

When examinating figs. 9b, 10b and 11b, which show the vorticity contribution from vertical advection of vorticity, we will find a very good agreement with the preliminary qualitative discussion, consequently areas of positive contribution where the warm air is ascending and cold air descending and *vice versa*. The meaning of this process is that we will get a weakening of the vorticity gradient across the frontal zone when the air is rising in both air masses, and a strengthening when the air is sinking. This may be equivalent with a weakening respectively a strengthening of the vorticity of the basic current. That problem has, for example, been discussed in a theoretical investigation by THOMPSON [10], where he shows that the change of total »rotationality» per unit time is approximately proportional to the vertical advection of vorticity:

$$\frac{1}{2}\overline{\frac{\partial}{\partial t}(\xi_1^2 + \xi_2^2)} \sim \frac{2}{3}\frac{R}{P}\overline{\omega \nabla^2 T} \quad (6.2)$$

Here ξ_1 = vorticity at a higher level ~ 400 mb, ξ_2 = vorticity at a lower level ~ 800 mb, P = pressure difference between level 1 and 2.

We must observe here that the mean operator has been taken over a closed area.

An examination of the two factors shows that they are non-correlated with respect to sign. It follows further that the absolute value of the twisting-term is in the mean only 1/3—1/2 of the vertical advection of vorticity (table 2). The difference is due to different degrees of truncation in the vertical advection term, the Laplacian of temperature is formed using the mesh length of d, whereas both of the first derivatives in the twisting-term have 2 d as mesh length. This has been pointed out by ARNASON and CARSTENSON [1]. The terms ought to be added before the finite differences are taken. An experiment with a denser grid-net shows that both terms are approximately inversely proportional to the grid-distance according to the dimensions of the frontal characteristics. Also the sum of the examined terms converges against zero as the region becomes larger. (The main result is, however, that we get a positive contribution to the vorticity development over the sea-level low as can be seen from table 1.)

Yet, the result is different from that obtained by Arnason and Carstenson, as these authors got a uniform sign for each term. This is not true in this study where we find that each of the term tends to balance itself over a larger area. This lack of agreement is presumably due to scale differences and also to departures in the technic of computation.

7. *Conclusions*

Because of the immense complexity of the development equation, great simplifications, as the assumption of a constant level of non-divergence and the use of vertical velocities computed from a »dry» adiabatic model, have been introduced in the computations of the different terms. Further, no account has been taken to geostrophic departures which presumably are very important in rapid cyclogeneses.

The lower boundary condition which states that $\omega = 0$ for $p =$ 1000 mb is also very bad in rapid developments because both $\frac{\partial p}{\partial t}$ and $\mathbf{v} \cdot \nabla p$ are different from zero. All these erroneous assumptions have involved inconsistencies in the treatment and especially the influences at the sea-level vorticity development arising from the vertical advection of vorticity and the twisting-term at the level of non-divergence

ought to be considered with some cautiousness. In spite of this, some conclusions may be stated with reference to this examined situation.

(1) Patterns of observed height changes at the 1000-mb level are in a general qualitative and a quantitative agreement with height changes computed from the vorticity and thermal advection, except in areas with strong descending motions. Before the cyclogenesis really takes place especially the vorticity advection is underrated because the level of non-divergence is situated higher up, according to PETTERSSEN [7] and MEANS [5] in the neighbourhood of the 300-mb level.

(2) When account also is taken to the buoyancy term the result deteriorates and the equation will probably not be able to predict cyclone development, especially in the early stage of the storm, unless respect is taken to the condensation heat by introducing the pseudoadiabatic lapse rate in areas with precipitation and/or clouds of precipitation.

(3) Vertical advection of vorticity through the level of non-divergence is presumably also important for the surface development especially if non-adiabatic vertical velocity is used, but another and more realistic boundary condition at the earth surface may complicate the contribution from this term very much.

Acknowledgments: The author wishes to express his thanks to Professor TOR BERGERON for his great interest in this problem and to Mrs. ANITA NILSSON for drawing the maps.

REFERENCES

1. ARNASON, G. and L. P. CARSTENSON, 1959: The effects of vertical vorticity advection and turning of the vortex tubes in hemispheric forecasts with a two-level model. *Mon. Weath. Rev.* **87**, 119—127.
2. BANNON, J. K., 1948: The estimation of large-scale vertical currents from the rate of rainfall. *Ouart. J. roy. Meteor. Soc.*, **74**, 57—66.
3. FJÖRTOFT, R., 1955: On the use of space-smoothing in physical weather forecasting. *Tellus*, **7**, 462—481.
4. FUGE, J. B. and J. B. KIPPER, 1957: An early-season snowstorm along the Atlantic coast, December 4—5, 1957. *Mon. Weath. Rev.*, **85**, 417—422.
5. MEANS, L. L., 1955: An investigation of cyclone development-storm of December 13—15, 1951. *Ibid.*, **83**, 185—198.
6. —»— 1956: Some basic parameters associated with the flood rains at Chicago October 9—12 1954. *Ibid.*, **84**, 253—260.

7. PETTERSSEN, S., 1955: A general survey of factors influencing development at sea level. *J. Meteor.*, **12**, 36—42.
8. —»— G. E. DUNN and L. L. MEANS, 1955: Report of an experiment in forecasting of cyclone development. *Ibid.*, **12**, 58—67.
9. SUTCLIFFE, R. C., 1947: A contribution to the problem of development. *Quart. J. roy. Meteor. Soc.*, **73**, 370—383.
10. THOMPSON, P. D., 1959: Statistical aspects of the dynamics of quasi-nondivergent and divergent baroclinic models. *C. G. Rossby Memorial Volume*, 350—359.
11. VUORELA, L. A., 1956: A study of vertical velocity distribution in some jet stream cases over western Europe. *Geophysica*, **6**, 68—90.
12. WIIN-NIELSEN, A., 1959: On certain integral constraints for the time-integration of baroclinic models. *Tellus*, **11**, 46—59.

FIGURES

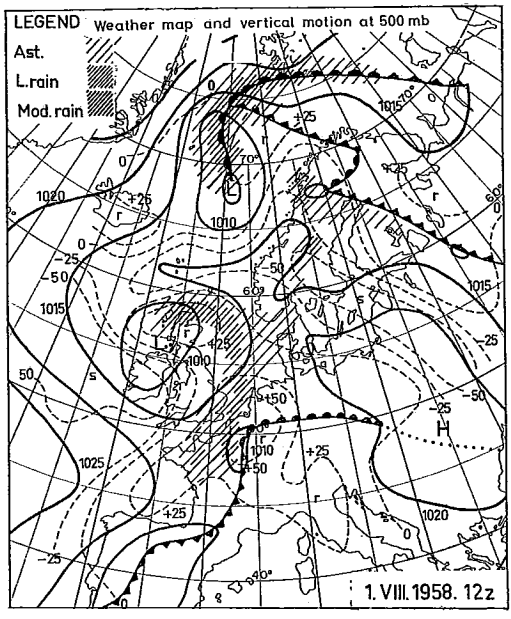

Figure 1. a) Surface chart with fronts for 1200 GMT, August 1, 1958. Surface isobars (solid lines) vertical velocity in mm/sec (dashed lines). *r* indicates core of ascending motion and *s* core of descending motion.

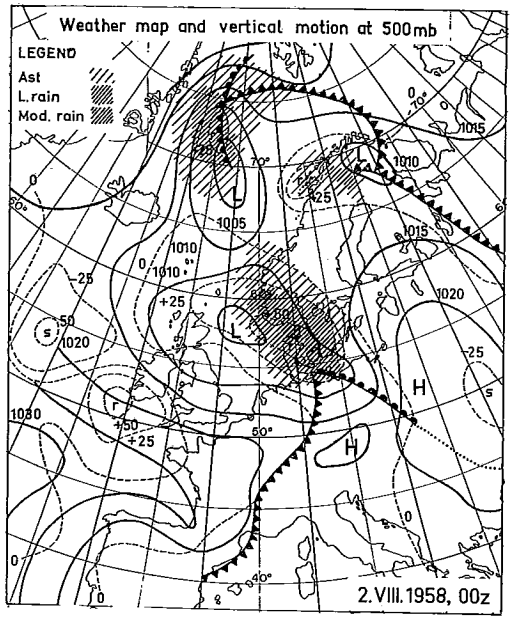

b) The same for 0000 GMT, August 2, 1958.

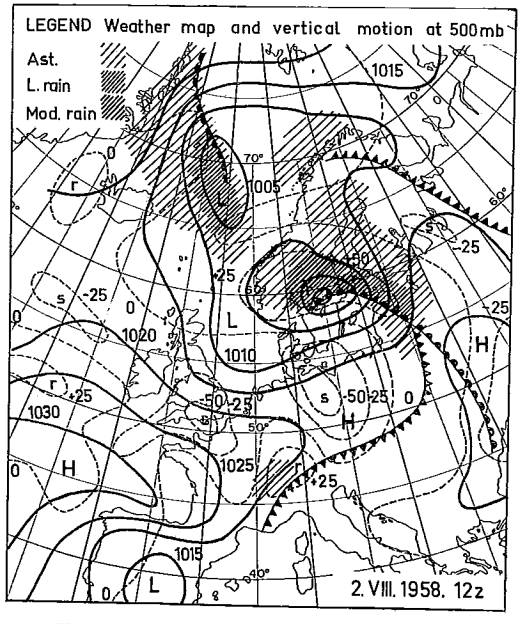

c) The same for 1200 GMT, August 2, 1958.

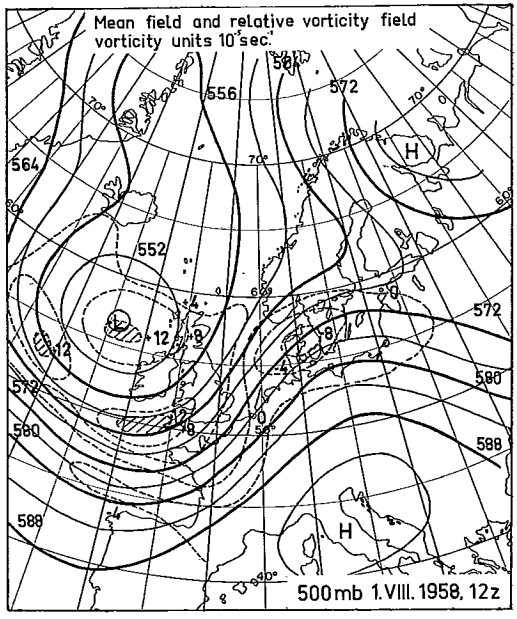

Figure 2. a) 500-mb height mean field (solid lines) and relative vorticity field (dashed lines) for 1200 GMT, August 1, 1958. In the mean field waves with wavelengths less than $6 \cdot 10^5$ m have been excluded. Units for the mean height field are dekam. and for the relative vorticity 10^{-5} sec^{-1}.

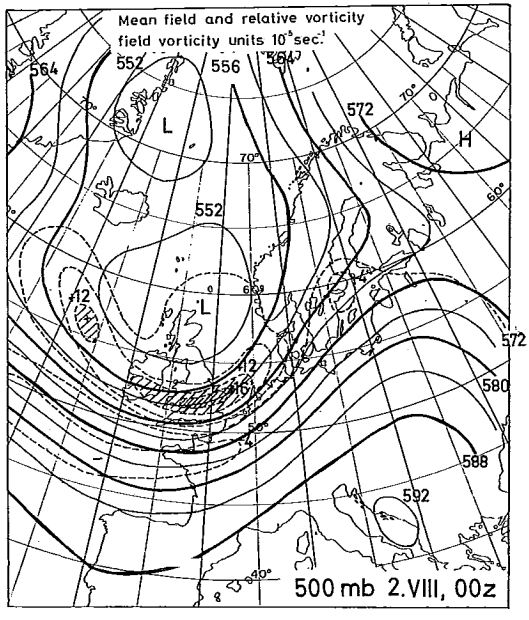

b) The same for 0000 GMT, August 2, 1958.

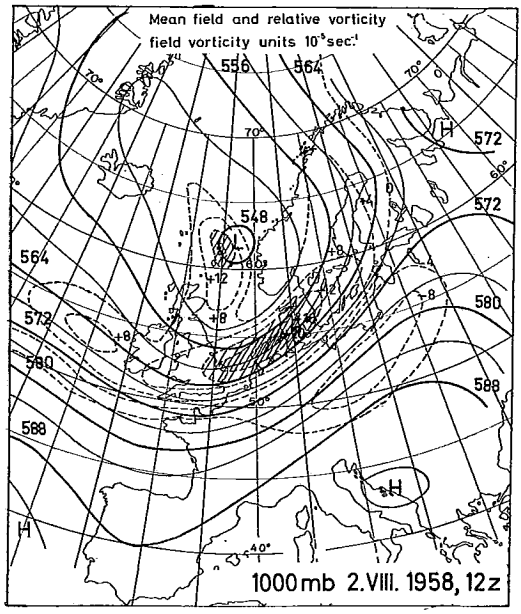

c) The same for 1200 GMT, August 2, 1958.

Figure 3. — 1200 GMT, August 1, 1958. a) Observed change of height for 1000-mb dekam. per 3 hours (solid lines). 1000-mb height field (dashed lines).

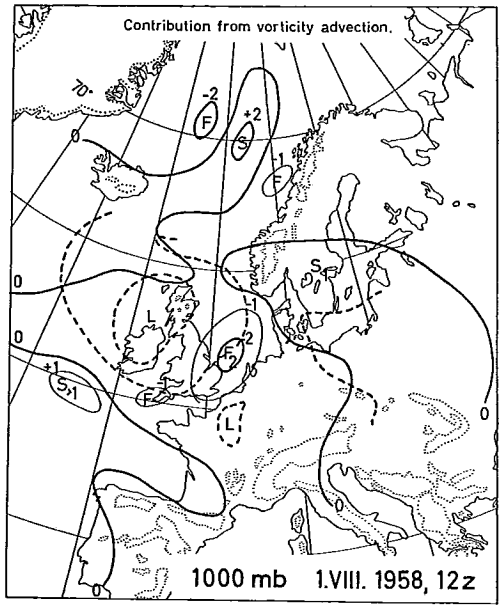

b) Contribution from vorticity advection in dekam. per 3 hours (solid lines). 1000-mb height field (dashed lines).

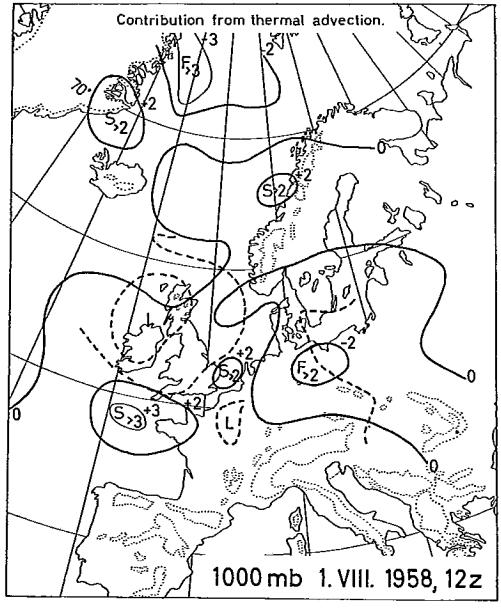

c) Contribution from thermal advection in dekam. per 3 hours (solid lines). 1000-mb height field (dashed lines).

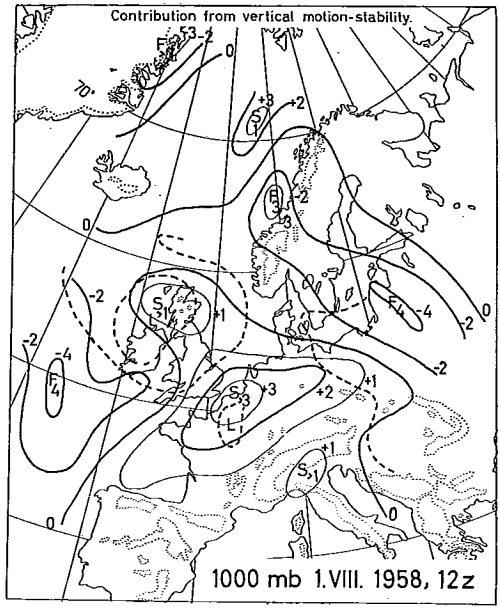

d) Contribution from vertical motion-stability in dekam. per 3 hours (solid lines). 1000-mb height field (dashed lines).

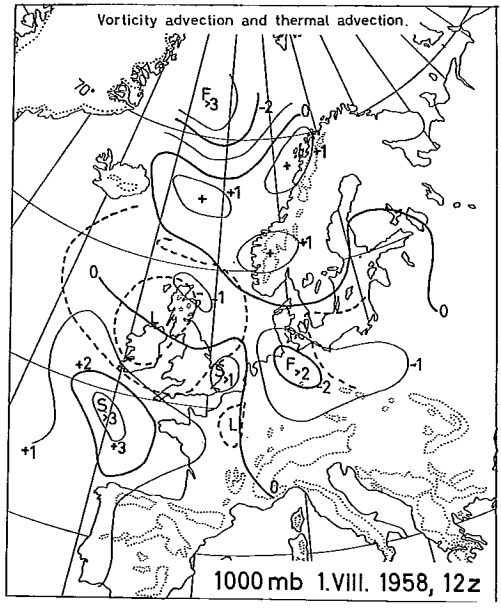

e) Contribution from vorticity advection and thermal advection in dekam. per 3 hours (solid lines). 1000-mb height field (dashed lines).

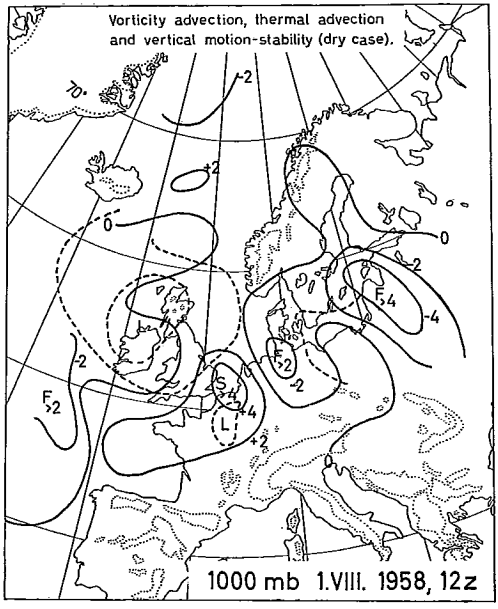

f) Contribution from vorticity advection, thermal advection and vertical motion-stability (dry case) in dekam. per 3 hours (solid lines). 1000-mb height field (dashed lines).

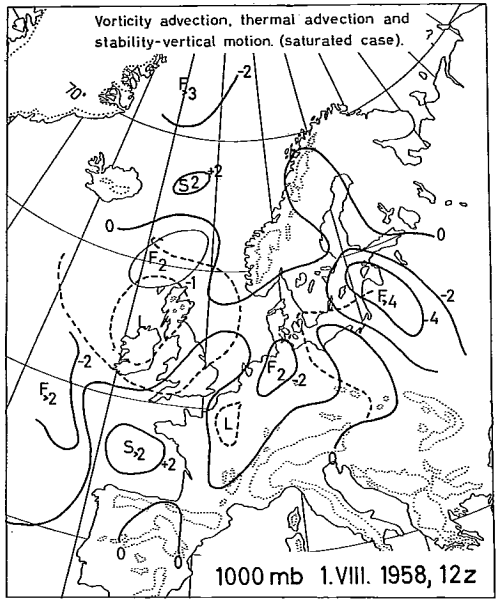

g) Contribution from vorticity advection, thermal advection and vertical motion-stability (saturated case) in dekam. per 3 hours (solid lines). 100-mb height field (dashed lines).

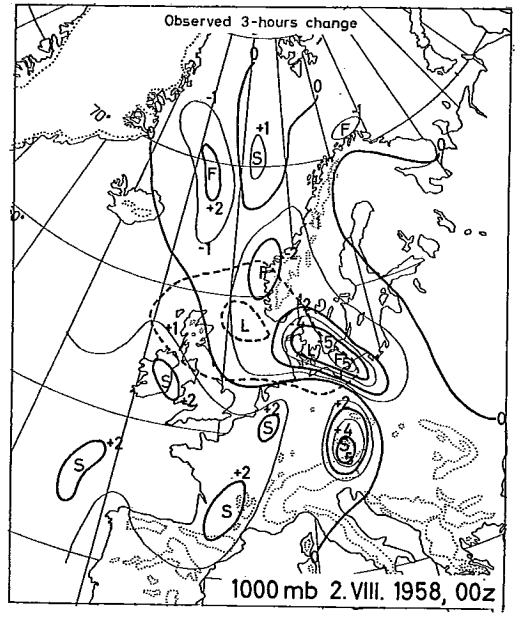

Figure 4. — 0000 GMT, August 2, 1958. a) The same as for figure 3.

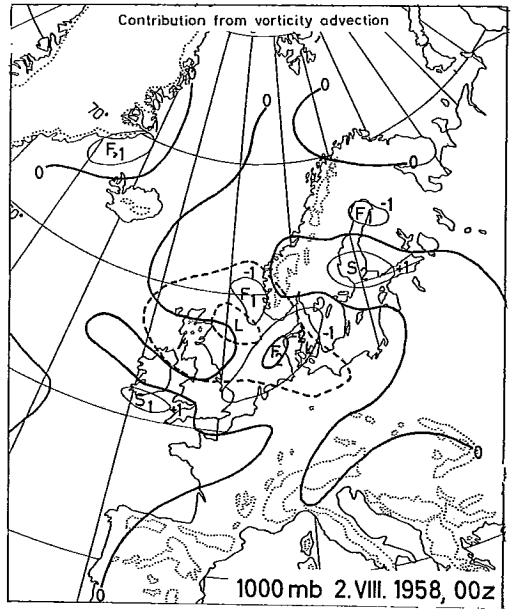

b) The same as for figure 3.

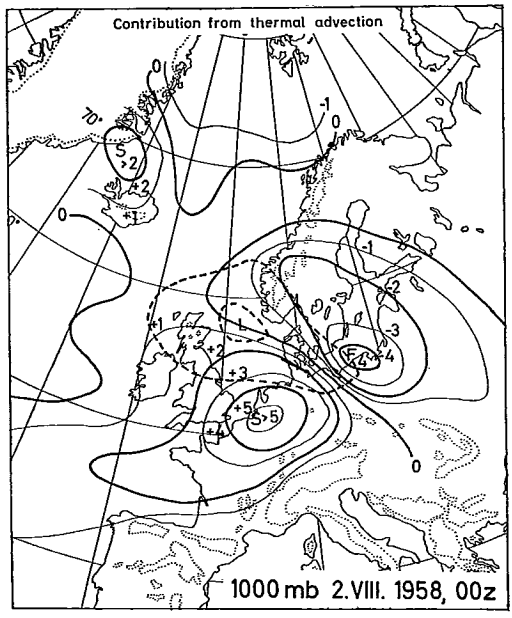

c) The same as for figure 3.

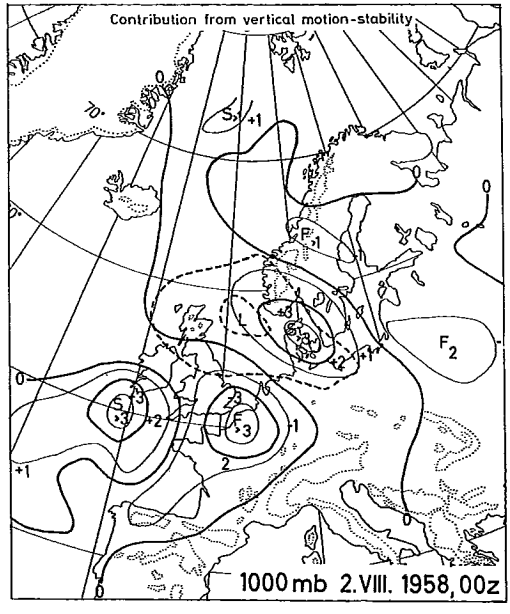

d) The same as for figure 3.

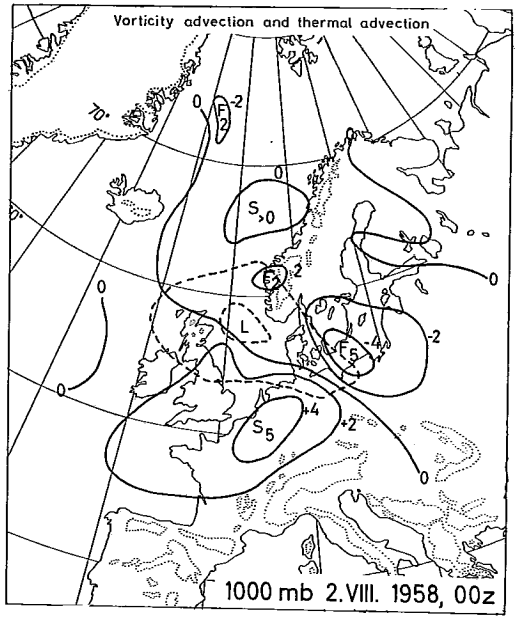

e) The same as for figure 3.

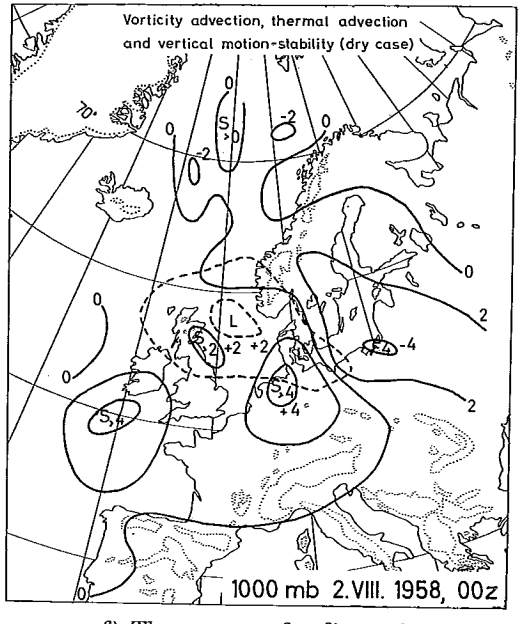

f) The same as for figure 3.

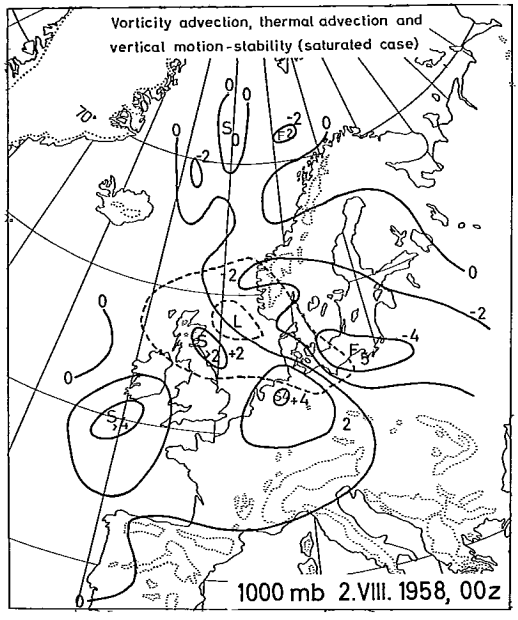

g) The same as for figure 3.

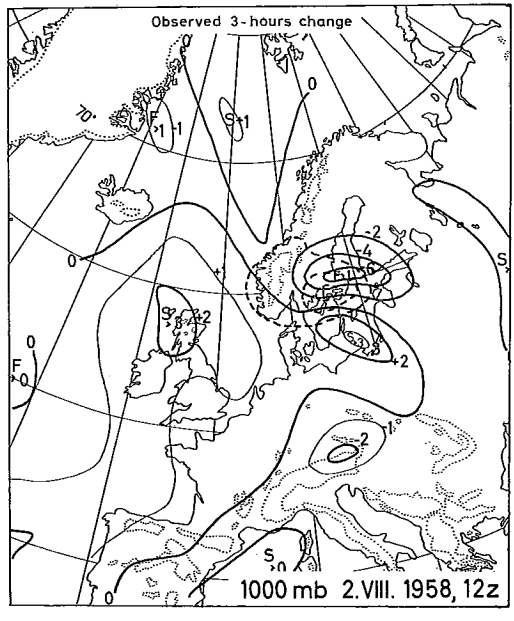

Figure 5. — 1200 GMT, August 2, 1958. a) The same as for figure 3.

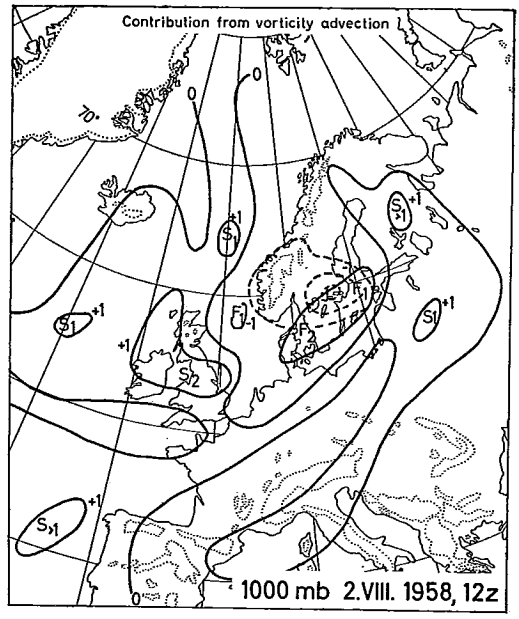

b) The same as for figure 3.

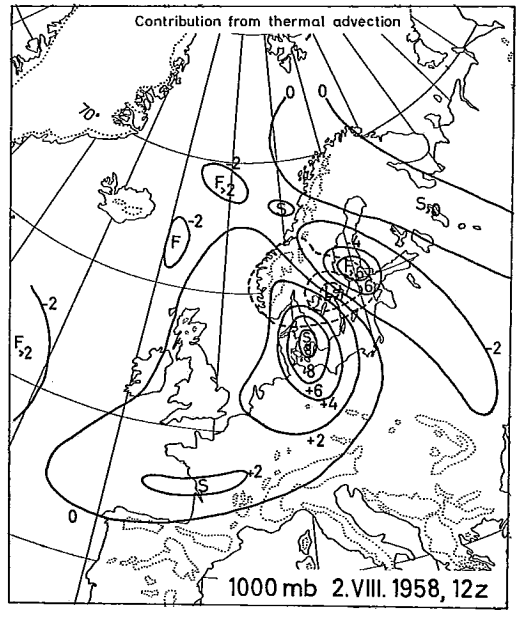

c) The same as for figure 3.

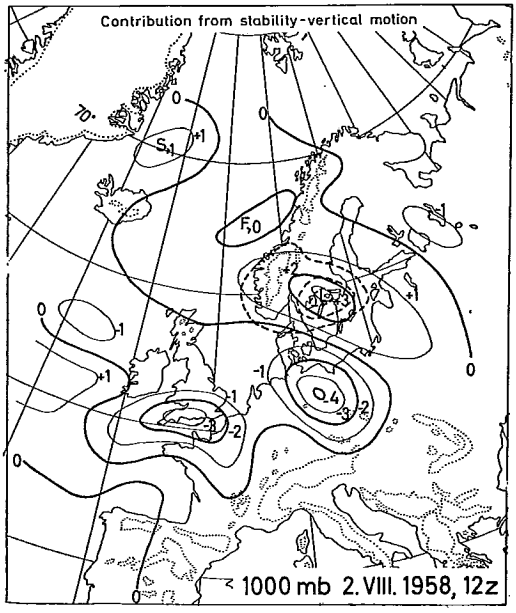

d) The same as for figure 3.

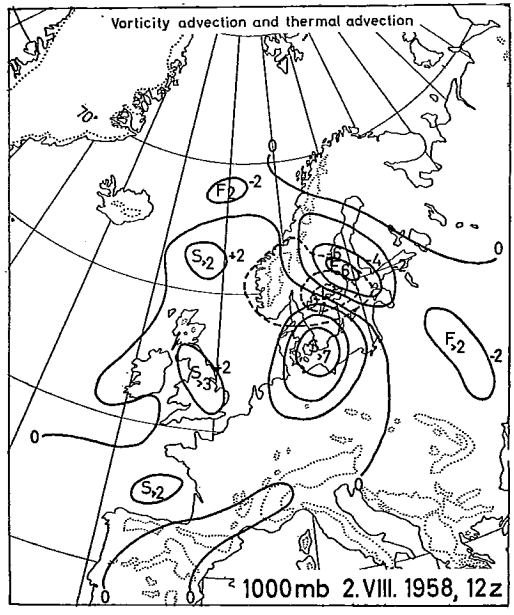

e) The same as for figure 3.

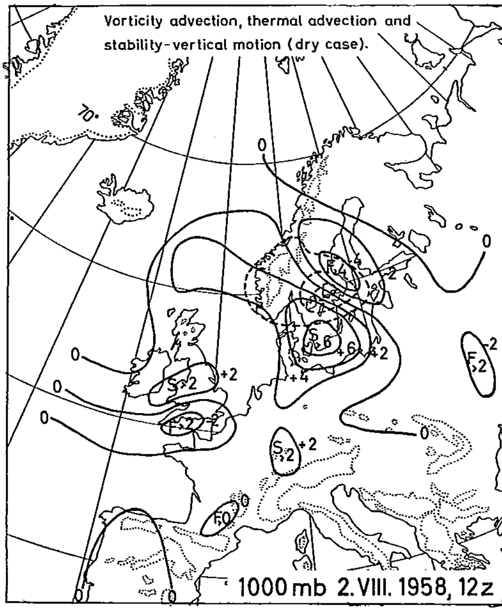

f) The same as for figure 3.

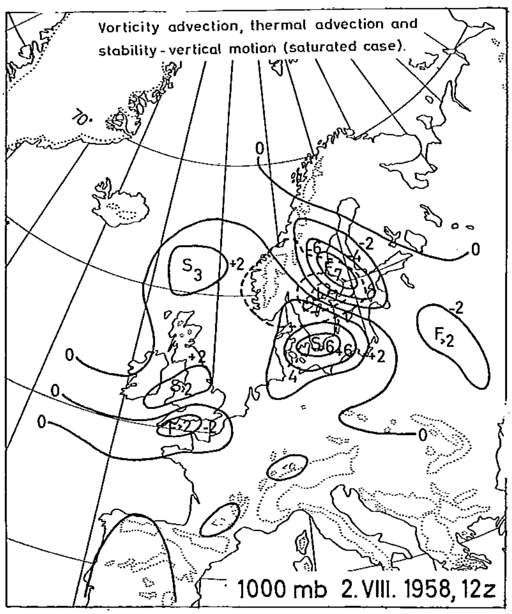

g) The same as for figure 3.

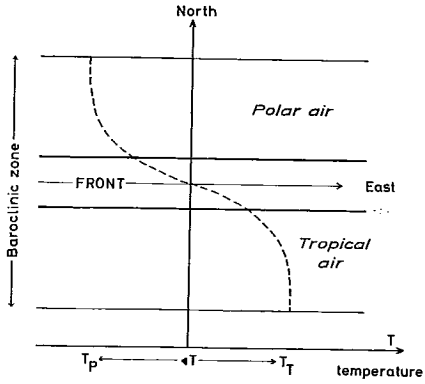

Figure 6. Front and a baroclinic zone in a horisontal plane with an idealized temperature curve. It is assumed that we have polar air to the north of the front (upper part of the picture) and tropical air to the south (lower part of the picture). The polar front is indicated by heavy solid lines, the baroclinic zone by solid lines and the temperature curve by a dashed line.

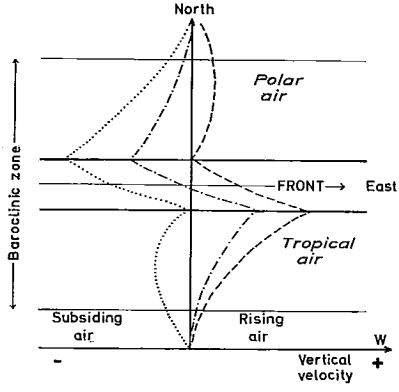

Figure 7. Front and a baroclinic zone in a horisontal plane with 3 idealized curves for the vertical velocity profile in connection with the polar front. It is assumed that we have polar air to the north of the front (upper part of the picture) and tropical air to the south (lower part of the picture). The polar front is indicated by heavy solid lines, the baroclinic zone by solid lines and the temperature curve by a dashed line. To the left of the y-axis we have sinking motion and to the right ascending motion. The dotted curve indicates a front with descending air in both air masses, the dotted — dashed curve a front with ascending warm air and descending cold air and the dashed curve a front with ascending air in both air masses.

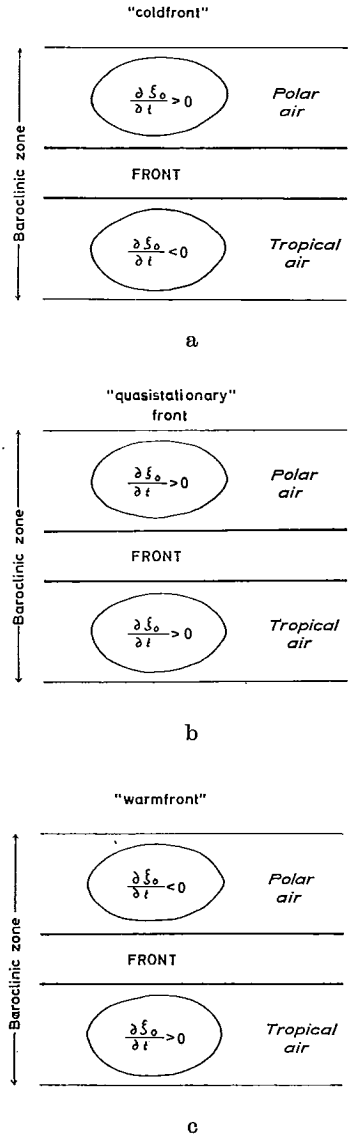

Figure 8. The vorticity contribution from the vertical advection term. The computation is based upon the assumption described under fig. 6 and fig. 7. 8a is computed from the vertical profile indicated by the dotted line in fig. 7, 8b from the vertical profile indicated by the dotted-dashed line in fig. 7 and 8c from the vertical profile indicated by the dashed line in fig. 7.

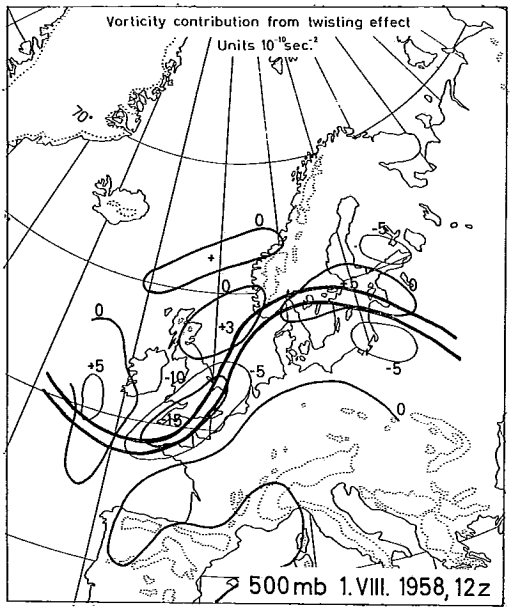

Figure 9. — 500-mb 1200 GMT, August 1, 1958. a) Vorticity contribution from the twisting effect (solid lines).

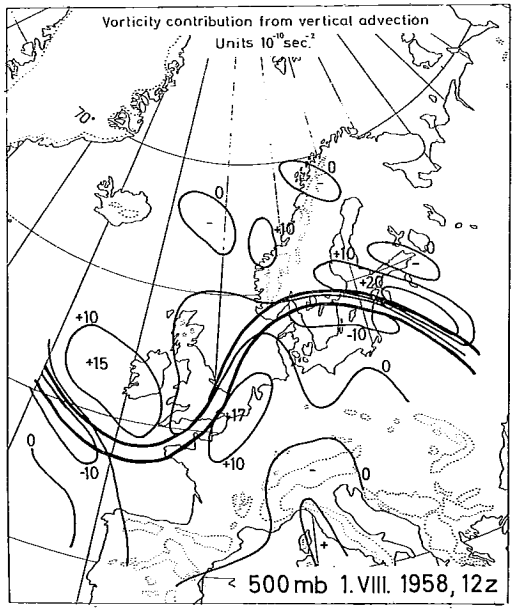

b) Vorticity contribution from vertical advection term (solid lines).

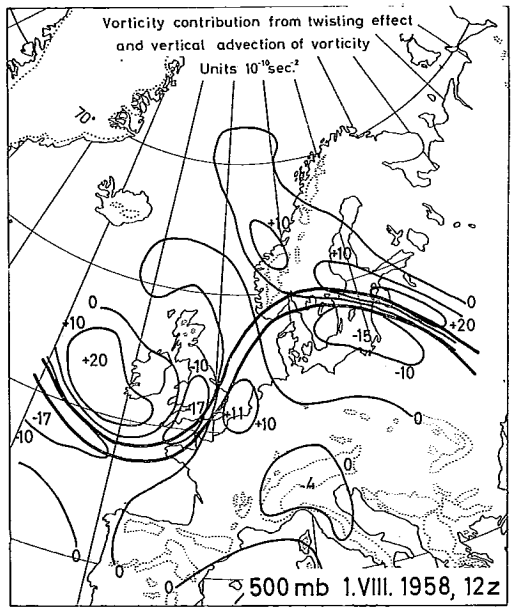

c) Vorticity contribution from twisting effect and vertical advection of vorticity (solid lines). Polar front (heavy solid lines). Units 10^{-10} sec^{-2}.

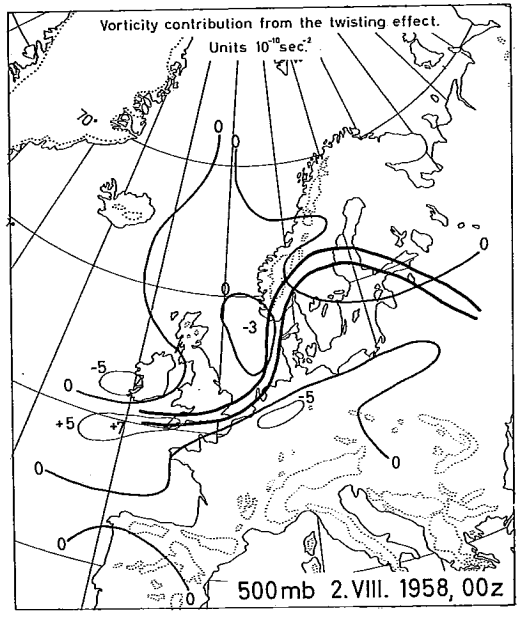

Figure 10. — 500-mb 0000 GMT, August 2, 1958. a) Vorticity contribution from the twisting effect (solid lines).

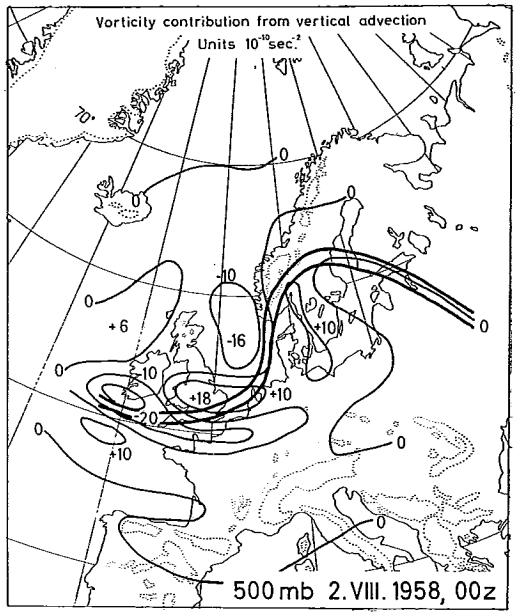

b) Vorticity contribution from vertical advection term (solid lines).

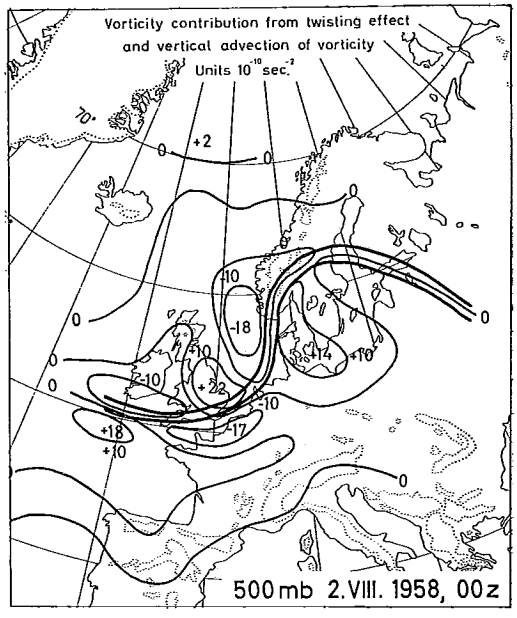

c) Vorticity contribution from twisting effect and vertical advection of vorticity (solid lines). Polar front (heavy solid lines). Units 10^{-10} sec^{-2}.

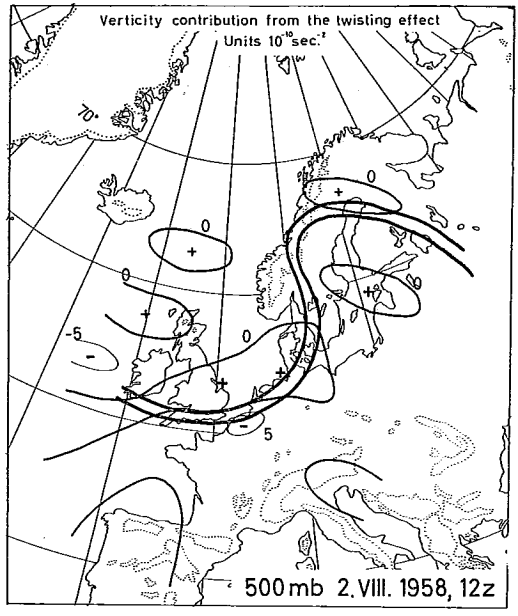

Figure 11. — 500-mb 1200 GMT, August 2, 1958. a) Vorticity contribution from the twisting effect (solid lines).

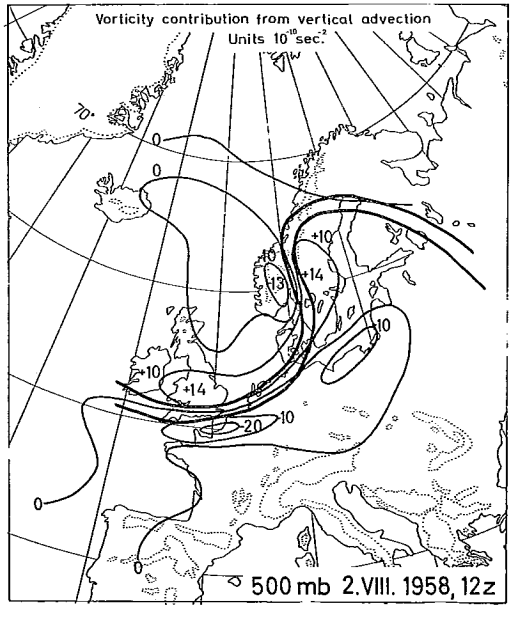

b) Vorticity contribution from vertical advection term (solid lines).

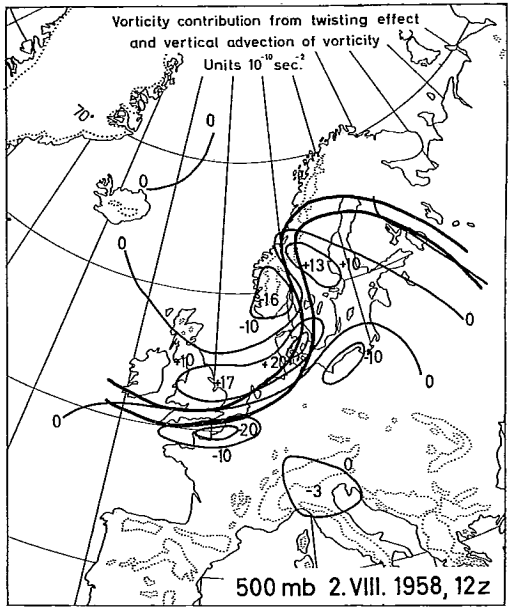

a) Vorticity contribution from twisting effect and vertical advection of vorticity (solid lines). Polar front (heavy solid lines). Units 10^{-10} sec^{-2}.